Joint Special Interest Group meeting between euspen and ASPE
Advancing Precision in Additive Manufacturing
Ecole Centrale de Nantes, France, September 2019
www.euspen.eu

Influence of the particle size distribution on surface quality of Maraging 300 parts produced by Laser Powder Bed Fusion

Mirko Sinico[1,2], Ann Witvrouw[1,2], Wim Dewulf[1]

[1]*Department of Mechanical Engineering, KU Leuven, 3001 Leuven, Belgium*
[2]*Member of Flanders Make - Core lab PMA-P, KU Leuven, 3001 Leuven, Belgium*

mirko.sinico@kuleuven.be

Abstract

This work investigates the effect of the powder particle size distribution on the surface finish of Maraging 300 specimens, produced by the Laser Powder Bed Fusion (LPBF) process. Although it is recognized that the initial powder morphological characteristics play an important role on LPBF part density, mechanical properties and surface quality, there is a lack of empirical data that could help to link the powder properties to actual metrological established surface parameters, like R_a or S_a. For this reason, an extensive initial powder characterization is presented in this paper, for three Maraging 300 batches, and first insights on the different obtained LPBF surface quality are disclosed. The results demonstrate how small differences in particle size distribution can decrease the LPBF surface roughness consistently. Moreover, it is shown how the use of fine powder can unlock novel LPBF processing strategies to further improve surface finish, down to 1.5 µm measured R_a, and thus reduce eventual post-processing efforts.

Powder Characterization, Powder Flowability, Surface Roughness, Laser Powder Bed Fusion (LPBF), Laser Polishing, Laser Remelting

1. Introduction

The improvement of the surface quality of parts produced by Laser Powder Bed Fusion is a critical topic of research in order to reduce further post-processing. LPBF is increasingly being used for the rapid manufacturing of parts and tools, e.g. injection mold inserts, where roughness values lower than 0.1 µm R_a can be required for critical surfaces. Typically, surface quality improvements are achieved by studying and tuning the effect of different LPBF processing parameters like laser scan strategy, layer thickness, laser power and laser scan speed [1,2,3]. It is likewise widely accepted that the characteristics of the LPBF starting material, e.g. powder particle shape and the powder particle size distribution (PSD), can have a significant effect on part density, mechanical properties and surface quality [3,4].
However, related to the effects on surface finish, only few literature studies, involving a limited palette of materials and often with non-sufficiently in-depth analysis of the initial powder morphology, exist on the subject. Previous studies on the influence of PSD on LPBF manufacturing for 316L [5,6] have highlighted how an amount of fine particles is beneficial, with an increased powder packing in the deposited LPBF layer and a diminished surface roughness on the produced parts. On the other side, finer powders can present a lower flowability which could hinder their deposition and therefore a limit exists on the smaller usable PSD. This limit not only is controlled by the average particle dimension, but also by the skewness and kurtosis of the PSD, where e.g. narrow distributions typically promote higher flowability [4].
In this paper, a first investigation of the influence of PSD variability on the surface roughness of Maraging 300 material is presented, with a prior extensive analysis on the powder characterization step and its flowability limit dependent on the PSD for three different powder batches. Subsequently, results on the surface roughness of LPBF produced specimens are discussed (section 4.2). Finally, a novel production strategy for fine powder distributions is disclosed, combining surface remelting with layer thicknesses as low as 10 µm to further reduce the top surface roughness (section 5).

2. Powder characterization

Maraging 300 powders with different PSDs have been acquired from the same supplier and fully characterized. The hereby called Mar 15-45 is the standard powder being sold for the LPBF process. The Mar 10-30 and Mar 5-15 have been engineered in collaboration with the supplier to meet specific constraints on the PSD. Specifically, the mean particle diameter was reduced with steps of 10 µm while also the span of the distribution (D10-D90) decreased with almost the same step, to promote the flowability. The difference is clearly observed in the laser diffraction (LD) analyses (Figure 1) for which measurements were performed via a Beckman Coulter LS 13 320 particle size analyser in dry mode, compliant to the ISO 13320:2009 standard.

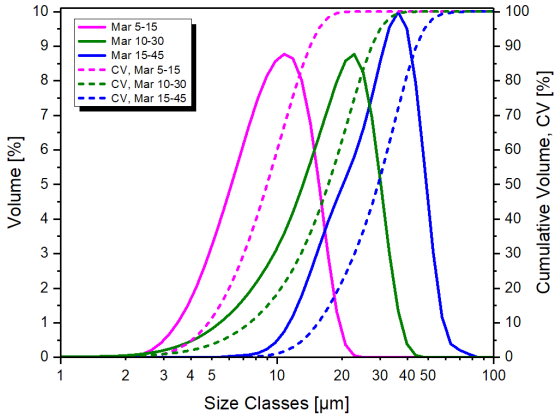

Figure 1. Laser diffraction analysis of the three acquired Maraging 300 powders, with PSD and cumulative PSD.

A summary of the LD analysis is also presented in Table 1, together with an overview of particles mean circularity and mean sphericity measured respectively with a KEYENCE Digital Microscope VHX-6000 and a Nikon X-ray Computed Tomography (CT) system XTH 225ST. Further details on the micro CT measurement of the powders can be retrieved in [7] and are not discussed in this paper. Definitions and an in-depth review on powder particles shape analyses can be found in [8].

Table 1. Laser diffraction numerical results of the three acquired Maraging 300 powders, together with mean circularity and mean sphericity from microscopic and tomographic investigations.

	D10 [µm]	D50 [µm]	D90 [µm]	Circularity, mean [-]	Sphericity, mean [-]
Mar 15-45	15.50 ± 0.78	29.29 ± 0.88	44.04 ± 2.20	0.800 ± 0.100	0.958 ± 0.025
Mar 10-30	7.48 ± 0.37	17.26 ± 0.52	27.34 ± 1.37	0.861 ± 0.098	0.962 ± 0.025
Mar 5-15	4.82 ± 0.24	8.99 ± 0.27	14.20 ± 0.71	0.849 ± 0.087	0.951 ± 0.027

**Note: circularity and sphericity are reported with measured standard deviation; LD statistics are reported with the theoretical coefficient of variation (COV) inferred from the ISO 13320:2009 standard.*

Measured circularity and sphericity are comparable between the different batches of powders and, consequently, the differences in PSD are presumed to influence predominately the surface quality of LPBF parts produced with these raw materials. Finally, before LPFB processing, the flowability (Hall Flow for 50 g of powder), apparent density ρ_{app} and tap density ρ_{tap} have also been acquired for all three powders following respectively the ASTM B213, B212 and B527 standards. Table 2 summarizes those results with the calculated Hausner Ratio HR (ρ_{tap}/ρ_{app}). The true density ρ_{true} is assumed to be 8.1 g/cm^3 for Maraging 300 as per supplier's datasheet.

Table 2. ASTM compliant measurements of flowability, ρ_{app}, ρ_{tap} and computed HR of the three acquired Maraging 300 powders.

	Hall Flow, 50 g [s]	ρ_{app} / ρ_{true} [%]	ρ_{tap} / ρ_{true} [%]	Hausner Ratio [-]
Mar 15-45	14.64 ± 0.23	52.3 ± 0.3	60.2 ± 0.1	1.15
Mar 10-30	No flow	48.9 ± 0.2	58.8 ± 0.1	1.20
Mar 5-15	No flow	39.7 ± 0.3	55.1 ± 0.1	1.39

**Note: all measurements reported with standard deviation*

A good flowability is necessary to be able to spread the powder in thin layers during LPBF production. The powder flow is a property influenced by many parameters, like PSD, particles shape, moisture, Van der Waals forces, magnetism, etc [3,4]. As a rule of thumb, a Hausner Ratio greater than 1.25 is considered to be an indication of poor flowability [4] and therefore it can be assumed that the Mar 5-15 will not be suitable for LPBF processing. At the same time, it is worth noticing that the Mar 10-30 powder batch, even with an inconclusive Hall Flow measurement, still presents a HR well below the suggested critical threshold.

3. LPBF specimens production and characterization methods

A 3D Systems ProX DMP 320 (rev. A, laser spot size ~60 µm) LPBF machine has been used for the fabrication of all the specimens in this work. Build plates with arrangements of samples ~20x10x10 mm have been processed with Mar 15-45 and Mar 10-30 powders, while the finer Mar 5-15 distribution has been discarded after multiple failed jobs. As predicted by the Hausner Ratio, the low flowability as well as particles agglomeration of the Mar 5-15 powder hinders the formation of an even powder layer during LPBF manufacturing. The use of a different recoating system than the equipped rubber blade, like the rotating roller, could eventually improve powder dispersion [3] but has not yet been tested.

After production, the relative density of the samples have been measured using Archimedes' principle. Subsequently, R_a roughness analyses have been collected on top and side surfaces by a Mitutoyo Formtracer CS-3200S4 profilometer, equipped with a 60° conic probe ending in a 2 µm diameter ball, following the ISO 4287:1997 standard. Each measurement reported in this work has been repeated 5 times at different locations on each specimen, taking care that the profiles are measured perpendicular to the typical lay lines featured on AM surfaces, i.e. the laser line tracks. For results with R_a above 10 µm, 2 sampling lengths have been collected instead of 5 (suggested value in the ISO standard) given the limited dimension of the specimens. It is anyhow assumed, from previous literature on LPBF measured roughness [9], that 2 sampling lengths i.e. R_{a2} (16 mm) are enough to obtain a good estimation of the R_a value. SEM inspection of selected specimens has been performed with a Philips XL 30 FEG, while qualitative optical investigations are done with a KEYENCE Digital Microscope VHX-6000.

4. Results and discussion

4.1. LPBF parameters optimization

Parameters optimization has been based on previous published work on the LPFB processability of Maraging 300 from our research group [10] and available literature [1,11]. For this comparison, samples have been fabricated at 3 different volumetric energy densities E_v ($= \frac{P}{v \times h \times t}$ with P laser power, h hatch spacing, t layer thickness), varying laser scanning speed and laser power while keeping hatch spacing and layer thickness fixed at 70 µm and 30 µm respectively. Striped pattern hatching, with 90° rotation between layers, and a single contour were also kept fixed. The same DoE has been repeated identically twice, once with the Mar 15-45 powder and once with the Mar 10-30. A summary of the DoE with the results on the Archimedes relative densities of the samples is presented in Figure 2.

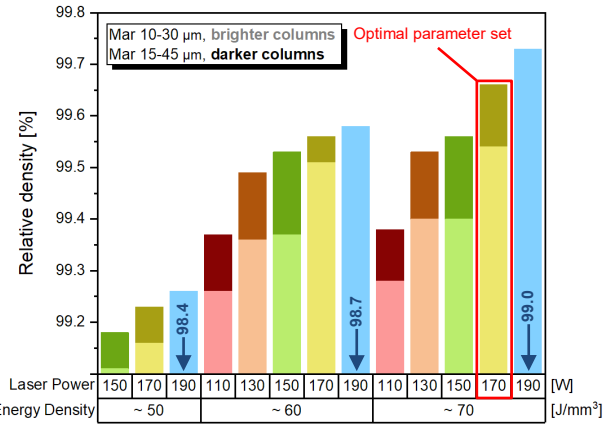

Figure 2. Relative densities of specimens fabricated from Mar 10-30 and Mar 15-45 powder batches, compared with the same repeated DoE.

As expected, the relative density increases for an increase in E_v or for an increase in laser power at the same E_v. This trend is valid, in the investigated parameters window, for both powder distributions. It must be noticed however that the relative density of the Mar 15-45 specimens suddenly start to decrease at 190 W laser power. It is hypothesized that, at this threshold,

the laser melting mode changes from conduction to keyhole eventually leading to keyhole voids and an increase in the total porosity content [12].
The Mar 10-30 specimens do not present this behaviour, even if their mean relative densities are slightly lower than the Mar 15-45 counterpart. It is generally believed that a fine powder granulation leads to higher relative densities. A narrow spread of the PSD is on the other hand reported as detrimental [3,4] because it lowers the apparent density ρ_{app} of the powder (as quantified in Table 2). A comprehensive weighted model of the two influencing factors has not yet been established, and therefore we can only assume that, for this study, the narrower PSD of the Mar 10-30 powder as well as fine particles vaporisation upon melting could be the cause for the slightly higher porosity content.
If a parameter set has to be chosen after the optimization, it is suggested to operate at 170 W, ~70 J/mm^3 E_v (1150 mm/s scan speed) for both the Maraging powders, as highlighted in Figure 2. The volumetric energy density with this optimal combination of parameters is in line with previously reported studies [1,11].

4.2. Surface roughness comparison

The top surface roughness of the produced specimens, according to the designed DoE, has been measured and plotted in Figure 3.

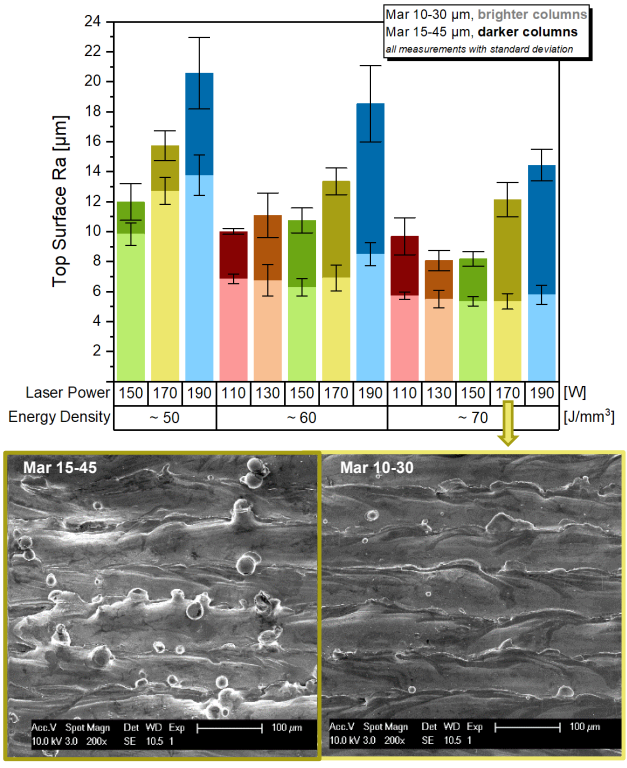

Figure 3. Top surface roughness of the specimens fabricated from Mar 10-30 and Mar 15-45 powder batches, compared with the same repeated DoE; for 170 W, 70 J/mm^3 E_v SEM pictures are also attached.

Top surface roughness is inversely proportional to the E_v, since at higher energy densities a more effective melting lowers the porosity content (Figure 2) and the amount of partially sintered particles. At the same time, surface roughness seems directly proportional to the laser power, at the same E_v, as increasing laser power results in larger and more turbulent melt-pools with an increased amount of spatter formation due to the lower melt viscosity and the higher degree of Marangoni effect [2,13].
Alongside, the influence of the PSD of the powder used to produce the specimens is appreciated at all levels of E_v or laser power. The specimens fabricated with the Mar 10-30 distribution presents a higher surface quality with a diminution of R_a from ~20 % to > 50 % compared to the Mar 15-45 samples. This effect is more pronounced at higher E_v, where R_a remains stable around 6 µm with its lowest value being at 170 W, 70 J/mm^3. SEM pictures for this combination of parameters are attached in Figure 3 for both Mar 10-30 (R_a of 5.34 µm) and Mar 15-45 (R_a of 12.12 µm). It is evinced again [3,4,5,6] how powders with fine granulometry are more substantially melted, leading to a more stable and continuous laser line track and a diminished balling effect and spatter formation.
A slightly lower R_a is also obtained for the side surfaces (90°) of the samples made from Mar 10-30 (Figure 4), even if the reduction is less evident and consistent being the staircase effect predominant in surface roughness contribution.

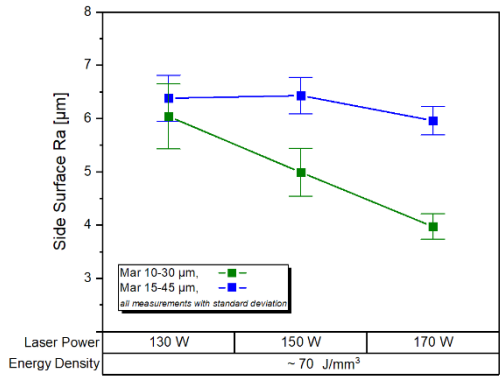

Figure 4. Example of side surface roughness of the specimens fabricated from the two powder batches, compared at the same E_v of 70 J/mm^3.

A more complete study should be carried out to understand how much the powder granulometry may influence the roughness of surfaces produced at different orientations in respect to the build platform.

5. A novel remelting strategy for the LPBF of fine powders

A common solution to decrease the surface roughness of the top surfaces in LPBF processing is the use of remelting [14]. With remelting, the already scanned layer is exposed once more to the laser radiation without new deposition of powder. The remelting step can be performed with the same LPBF processing parameters or it can be tuned (with different parameters) in accordance to the desired outcome needed, with a similar optimization approach that is found for laser polishing machines [15]. Multiple remelting passes are generally suggested to further improve the final surface quality, at the disadvantage of processing time.
It is likewise well established that reducing the processing layer thickness t usually improves the surface quality [13]. This improvement is mostly appreciated for side surfaces, with the diminished staircase effect, but top surfaces are affected too.
In the final part of this work we want to suggest a novel remelting strategy for top surfaces, where the last layers are first built with t of 10 µm and subsequently remelted. This approach basically combines the two positive effects of the remelting step and low t, but its successful implementation is constrained by the limits of the granulometry of the powder used and sometimes by LPBF machine limits. Fortuitously, the Mar 10-30 powder batch presents at least 50 vol% of the particles (D50) with a diameter around the effective layer thickness for t of 10 µm (t_{eff} = 16.67 µm for a powder layer density of 60 % [5]), and therefore is deemed suitable for testing the approach.
The DoE hereby explained is just a brief overview of the obtained results. In details, the last 90 µm of 20x10x10 mm specimens have been printed with a t of 10 µm followed by five remelting

steps (90° rotation each step) of the last layer. Parameters for the underlying part have been kept at the optimized combination reported in paragraph 4.1, while the parameters for the top 10 µm layers have been varied. Moreover, to compare the obtained R_a from the novel approach to a standard remelting step or decreased t alone, reference specimens with only the 5x remelting applied on the top surface or only the 10 µm reduced t for 90 µm have also been produced and measured. The outcomes of this brief trial are summarized and reported in Figure 5 for two E_v (calculated for t = 10 µm).

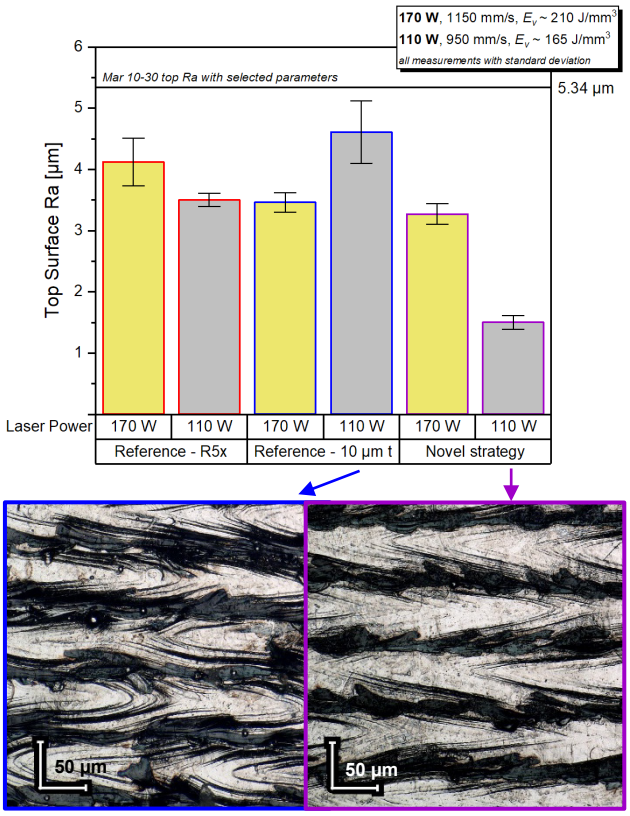

Figure 5. Measured R_a of the samples produced at R5x (top surface remolten 5 times), 10 µm t (last 90 µm of the specimens built with a layer thickness of 10 µm), and the combination of the two, for two E_v; sampling pictures from optical microscopy attached.

It is evinced how the single reference strategies alone provide little improvement from the already low R_a obtained with the Mar 10-30 specimens, while the combination of the two positive effects at a tuned E_v of ~165 J/mm³ is able to further reduce the surface roughness to a remarkable value of 1.5 µm.
With the initial reduced layer thickness step, we are able to decrease both the mean height of the profile elements in the roughness domain R_c, and their mean width RS_m. We believe that this reduction, even if it doesn't reflect in a significant decrease in R_a, is beneficial to prepare the surface for the last remelting step. To prove this hypothesis, full topographic measurements are currently being performed on a 3D optical profiler Sensofar S neox.

6. Conclusions

In this work preliminary results, linking the LPBF powder morphological characteristics to the LPBF surface quality, are disclosed for the first time for the Maraging 300 material. Through the extensive test of three different powder batches, it is evinced how a flowability limit exits dependent on the particle size distribution, and this limit will determine if the powder is suitable for LPBF processing. Furthermore, through the comparison of specimens produced with the used Mar 10-30 and Mar 15-45 powder distributions, it is demonstrated how a small difference in PSD towards finer particles can considerably improve the surface quality of fabricated parts with up to a > 50 % decrease in the evaluated R_a roughness parameter. Finally, the use of finer powder is not only positive for the general diminished R_a, but could as well unlock the possibility to adapt the LPBF scanning strategy to further enhance the surface finish. For this reason, a novel remelting strategy for the LPBF of fine powders has been tested, and was proven effective reaching the value of 1.5 µm R_a. Full topographic measurements are currently being performed to better understand the developments of surface texture.

Acknowledgements

This research was funded by The EU Framework Programme for Research and Innovation - Horizon 2020 - Grant Agreement No 721383 within the PAM² (Precision Additive Metal Manufacturing) research project.

References

[1] Casalino G, Campanelli S L, Contuzzi N and Ludovico A D 2015 Experimental investigation and statistical optimisation of the selective laser melting process of a maraging steel *Optics & Laser Technology* **65** 151-158
[2] Derahman N A, Karim M S, and Amran N A M 2018 Effects of process parameters on surface quality of parts produced by selective laser melting - ANFIS modelling *Proceedings of Mechanical Engineering Research Day 2018* 115-116
[3] Malekipour E and El-Mounayri H 2018 Common defects and contributing parameters in powder bed fusion AM process and their classification for online monitoring and control: a review *Int J Adv Manuf Technol* **95** 527-550
[4] Tan J H, Wong W L E and Dalgarno K W 2017 An overview of powder granulometry on feedstock and part performance in the selective laser melting process *Additive Manufacturing* **18** 228-255
[5] Spierings A B, Herres N and Levy G 2011 Influence of the particle size distribution on surface quality and mechanical properties in AM steel parts *Rapid Prototyping Journal* **17** 195-202
[6] Liu B, Wildman R, Tuck C, Ashcroft I, and Hague R 2011 Investigation the effect of Particle Size Distribution on processing parameters optimisation in Selective Laser Melting process *Proceedings of the Annual International SFF Symposium 2011*
[7] Sinico M, Ametova E, Witvrouw A, and Dewulf W 2018 Characterization of AM Metal Powder with an Industrial Microfocus CT: Potential and Limitations *Proceedings of the 2018 ASPE and euspen Summer Topical Meeting* **69** 286-291
[8] Sutton A T, Kriewall C S, Leu M C and Newkirk J W 2017 Powder characterisation techniques and effects of powder characteristics on part properties in powder-bed fusion processes *Virtual and Physical Prototyping* **12** 3-29
[9] Triantaphyllou A et al. 2015 Surface texture measurement for additive manufacturing *Surf. Topogr.: Metrol. Prop.* **3**
[10] Kempen K, Yasa E, Thijs L, Kruth J P and Van Humbeeck J 2011 Microstructure and mechanical properties of Selective Laser Melted 18Ni-300 steel *Physics Procedia* **12** 255-263
[11] Tan C, Zhou K, Kuang M, Ma W and Kuang T 2018 Microstructural characterization and properties of selective laser melted maraging steel with different build directions *Science and Technology of Advanced Materials* **19** 746-758
[12] King W E et al. Observation of keyhole-mode laser melting in laser powder-bed fusion additive manufacturing 2014 *Journal of Materials Processing Technology* **214** 2915-2925
[13] Bacchewar P B, Singhal S K and Pandey P M 2007 Statistical modelling and optimization of surface roughness in the selective laser sintering process *Proceedings of the Institution of Mechanical Engineers, Part B: Journal of Engineering Manufacture* **221** 35–52
[14] Yasa E, Deckers J, and Kruth J 2011 The investigation of the influence of laser re-melting on density, surface quality and microstructure of selective laser melting parts *Rapid Prototyping Journal* **17** 312–327
[15] dos Santos Solheid J, Jürgen Seifert H, and Pfleging W 2018 Laser surface modification and polishing of additive manufactured metallic parts *Procedia CIRP* **74** 280–284